Appl. Phys. B 84, 507–510 (2006)
DOI: 10.1007/s00340-006-2284-0

Applied Physics B
Lasers and Optics

Y.W. CHEN[1,2]
Y.C. LIU[1,✉]
S.X. LU[3]
C.S. XU[1]
C.L. SHAO[1]

Photoelectric properties of ZnO: In nanorods/SiO_2/Si heterostructure assembled in aqueous solution

[1] Center for Advanced Optoelectronic Functional Material Research, Northeast Normal University, Changchun 130024, P.R. China
[2] Key Laboratory of Excited State Processes, Changchun Institute of Optics, Fine Mechanics and Physics, Chinese Academy of Sciences, Changchun 130033, and Graduate School of the Chinese Academy of Sciences, P.R. China
[3] Department of Chemistry, School of Science, Beijing Institute of Technology, Beijing 100081, P.R. China

Received: 20 January 2006/Revised version: 25 April 2006
Published online: 8 June 2006 •

ABSTRACT In-doped zinc oxide (ZnO:In) nanorods were grown onto SiO_2/n-Si substrate without catalyst in aqueous solution. The ZnO:In nanorods/SiO_2/n-Si heterostructure photovoltaic device was prepared. The structural and photoelectric properties of the as-grown ZnO:In nanorods were analyzed. ZnO:In nanorods had a strong and broad UV surface photovoltage response in the range of 300–400 nm, and the bands were identified. The photoelectric conversion properties of ZnO:In nanorods/SiO_2/n-Si heterostructure were investigated. ZnO:In/SiO_2/n-Si heterostructure showed a wide range photocurrent spectral response with high intensity in the UV and visible region. The rectifying behavior of this heterostructure was observed. Moreover, the device had a low turn-on voltage and a high breakdown voltage. Current–voltage characteristic was studied for the heterostructure, and the open-circuit voltage and short-circuit current were obtained.

PACS 73.40.Lq; 85.35.Be; 81.16.Dn

1 Introduction

ZnO as a nontoxic direct wide-band-gap semiconductor with a large exciton binding energy (60 meV at room temperature) has aroused intensive research in recent years, especially its one-dimensional nanostructures [1–3]. This can be attributed to its peculiar and exceptional properties as a promising material for optical and electrical applications as solar cells, field-effect transistors, field emitters, transparent conducting windows, blue light emitting, etc. [4, 5]. However, how to organize these one-dimensional nanostructural materials into functional nanodevices is the most critical issue faced by researchers. The efficient carrier transport can be obtained in one-dimensional materials because of the decreasing grain boundaries, discontinuous interfaces and two-dimensional limited charge transport compared to the zero-dimensional nanocrystal materials. This will be favorable to obtain high performance nanodevices. Moreover, this efficient carrier transport can be used in the light-collecting devices, such as solar cells, etc. Especially, solution-processed ZnO nanorods provide a potential route to low-temperature assemble and high mobilities. These exceptional properties also provide a route to high performance inorganic semiconductor TFTs based on self-assembly of colloidal ZnO nanorods [6] and ordered ZnO nanorod-polymer photovaltic devices [7]. ZnO is a good candidate for substituting indium tin oxide (ITO) films in amorphous silicon solar cells because it is stable in hydrogen plasma ambient. ZnO coatings were used as high conductivity transparent front contact layers [8, 9] to facilitate current collection. The capability of photoelectric conversion is important for light-collecting devices. Multi-junctions [10–12] devices and dye-sensitized ZnO nanocrystals [13] polymer-inorganic semiconductor solar cells have been investigated depending on the photoelectric properties of ZnO. However, one-dimensional doped ZnO nanostructural heterojunctions for light-collecting applications have not been reported. In this work, ZnO:In nanorods were grown onto SiO_2/n-Si substrate in aqueous solution. The ZnO:In nanorods/SiO_2/n-Si heterostructure photovoltaic device was prepared. This method provides a possibility for low-temperature, large-scale production of nanodevices on flexible substrates. To enhance the n-type conductivity character of ZnO, n-type dopants (In) is chosen. The photoelectric properties of ZnO:In nanorods/SiO_2/n-Si heterostructure were investigated.

2 Experiments

All the chemicals are analytic grade reagents without further purification and from Beijing Chemical Company. The undoped and In-doped ZnO thin films were grown on SiO_2/n-Si(100) and quartz substrates, respectively, in aqueous solution [14]. The samples were prepared in the same condition. Zinc nitrate hexahydrate ($Zn(NO_3)_2 \cdot 6H_2O$) and methenamine ($C_6H_{12}N_4$) reacted in the condition of equimolar for 0.02 molar. Different substrates were placed vertically in one aqueous solution of 0.02-M $Zn(NO_3)_2 \cdot 6H_2O$ and 0.02-M $C_6H_{12}N_4$ in the glass bottles at 95 °C for 2 h. 0.0002-M Indium chloride ($InCl_3 \cdot 4H_2O$) acting as a dopant was mingled with the aqueous solution to produce ZnO:In nanorods. For ZnO:In nanorods/SiO_2/n-Si and

✉ Fax: (86)431-568-4009, E-mail: ycliu@nenu.edu.cn

$ZnO/SiO_2/n$-Si heterostructure, indium electrodes were thermally evaporated at the surface of ZnO:In, ZnO and the rear Si surface in order to establish the Ohmic contacts.

The X-ray diffraction (XRD) pattern were collected on a D/max-RA X-ray diffraction spectrometer (Rigaku) using Cu K_α radiation ($\lambda = 1.54$ Å) and scanning electron microscopy (SEM) was recorded by a Hitachi-600. For photoelectric characteristics, the surface photovoltage spectroscopy (SPS) measurements were performed with the SPS instrument [15]. Monochromatic light was obtained by passing light from a 500 W xenon lamp through a double-prism monochromator (Hilger and Watts, D 300). A lock-in amplifier, synchronized with a light chopper was employed to amplify the photovoltage signal. The optical-absorbtion spectra were recorded on a UV-vis spectrophotometer (Lamda 900, Perkin-Elmer) in the range of 200–500 nm. Spectral photocurrent response measurements were performed using a luminescence spectrophotometer (LS 55, Perkin-Elmer). The measuring region covers the range from 200 to 800 nm. Pulsed monochromatic light was used. The current–voltage characteristics of $ZnO:In/SiO_2/Si$ heterojunction were studied.

3 Results and discussion

The morphology and microstructure of the as-grown $ZnO:In/SiO_2/Si$ and $ZnO/SiO_2/Si$ were characterized and analyzed by SEM images shown in Fig. 1. Dense In-doped and undoped ZnO nanorods are observed. The as-grown samples have a similar size and uniform rodlike shape. These nanorods show a same length of approximately 3 μm and an average diameter of about 250 nm.

The XRD patterns of $ZnO:In/SiO_2/Si$ and $ZnO/SiO_2/Si$ samples are shown in Fig. 2. The diffraction peaks from (100), (002), (101) and (110) all appear in the XRD spectra. It demonstrates that the samples are typically hexagonal wurtzite structures. The major diffraction peaks shift slightly towards lower diffraction angle compared with the ZnO nanorods after In incorporation. According to Bragg diffraction formula $2d \sin\theta = n\lambda$, increasing of lattice constant indicates that In^{3+} (ionic radius of In^{3+} and Zn^{2+} are 0.08 nm and 0.074 nm, respectively) enters the lattice of ZnO. Where d is lattice constant, θ is diffraction angle, and λ is X-ray wavelength. Furthermore, it is also illustrated by the absorption spectra and surface photovoltage spectra.

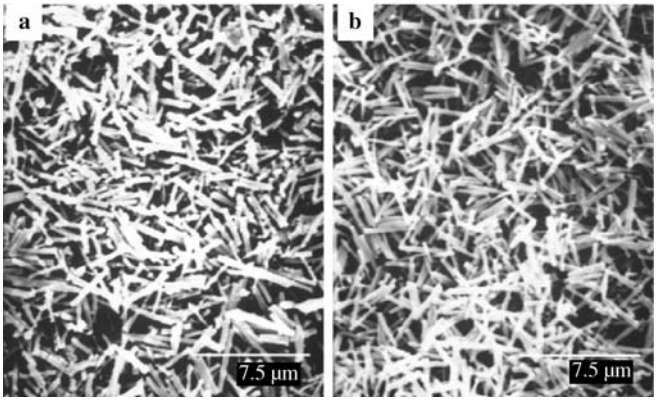

FIGURE 1 SEM images of the as-grown $ZnO/SiO_2/Si$ (**a**) and $ZnO:In/SiO_2/Si$ (**b**)

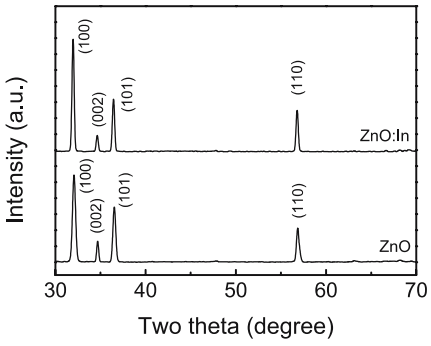

FIGURE 2 XRD spectra of $ZnO:In/SiO_2/Si$ and $ZnO/SiO_2/Si$ samples

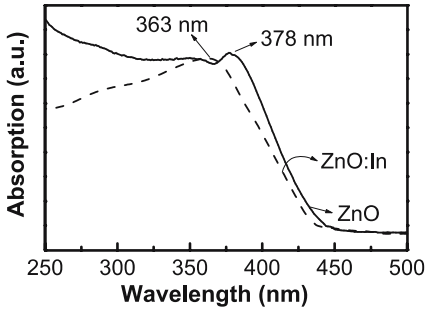

FIGURE 3 Optical-absorption spectra of In-doped and undoped ZnO nanorods

We measured the optical-absorption spectra of the two kinds of samples on quartz substrates, as shown in Fig. 3. In the UV region, some amount of tailing occurs in the band gap below the absorption edge. It means that there are impurity states, which can cause a perturbation of the band structure. The band-edge absorption can be ascribed to the fundamental absorption and defects absorption near the band-edge. Moreover, a pronounced exciton absorption peak is visible near the absorption edge for ZnO sample. However, the exciton absorption peak of ZnO:In is not obvious because of the dopant absorption near the band-edge range. The overlapping of the impurity absorption and exciton absorption results the broaden of the absorption peak. Exciton absorption peak position of ZnO and ZnO:In are 378 nm and 363 nm, respectively. Accordingly, the optical band gap should be calculated in terms of the equation $E_g = P_l + \Delta E_b$ [16] instead of $(\alpha h\nu) = C(h\nu - E_g)^{1/2}$ [17], where P_l and ΔE_b are the absorption peak position of exciton and the exciton binding energy, respectively. C is a constant, and α is optical-absorption coefficient. As a result, the optical-absorption band gap of ZnO:In is larger than that of pure ZnO (3.34 eV). The phenomenon should be attributed to the well-known Burstein–Moss shift [18] on the basis of the results of Hamberg and Chopra et al. [19, 20]. In addition, the shift of the optical band gap of ZnO also illustrates that indium incorporates into the ZnO crystal lattices, which accords with XRD results.

The formation of interface states can be proven by the measurement of SPS. To study the charge transfer properties in photo-stimulated surface interaction, the surface photovoltage (SPV) of ZnO:In and ZnO nanorods were investigated by SPS. The samples were obtained from the SiO_2/Si sub-

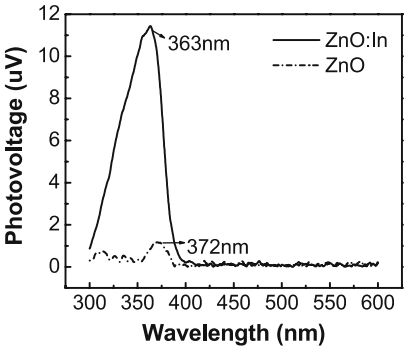

FIGURE 4 Surface photovoltage spectra of ZnO:In and ZnO nanorods

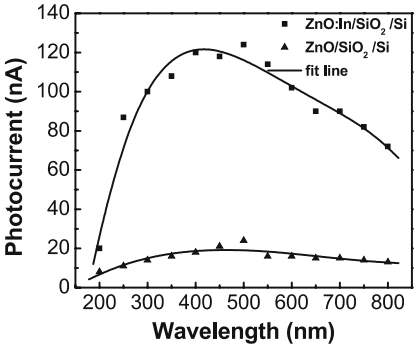

FIGURE 5 Photocurrent spectra of ZnO:In/SiO_2/Si, ZnO/SiO_2/Si heterostructures

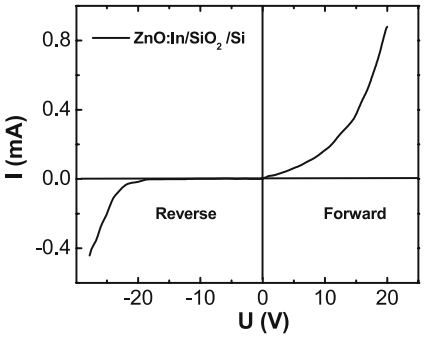

FIGURE 6 The I–V characteristic curve for ZnO:In/SiO_2/Si heterostructure

strates. SPS is an effective tool to investigate the photophysics of excited states generated by absorption in the aggregate state [21]. The SPS curves are shown in Fig. 4. The SPV response wavelengths locate in the UV region. One interesting phenomenon is that there is a broad photovoltaic response band in the range of 300–400 nm for ZnO:In. Furthermore, the SPV band range is consistent with UV-vis absorption region (Fig. 3) of ZnO:In sample. This suggests that the absorption band contributes to the SPV response. According to the SPV response wavelength region, we can conclude that this band comes from two different mechanism, band to band transition and exciton transition, respectively. Band to band transition in these spectra is situated in the wavelength range from 300 nm to above near-band-edge. Consequently, photogenerated electron–hole pairs possess higher energy. Exciton transition locating near-band-edge region should be attributed to the exciton pairs generated by excited donor surface states. ZnO are often n-type conduction, due to stoichiometric deviation. In the air, ZnO of n-type conduction can make part of the absorbed O_2 negatively charged, producing a built-in field at the surface of the as-grown nanorods [15]. The built-in field is so oriented that the outer surface is negative and the space charge region is positive. When the samples are illuminated by light of appropriate wavelength, the photogenerated electron–hole pairs are separated by the built-in field at the surface of ZnO:In sample, and contribute to the measured photovoltaic response. The surface photovoltaic response intensity of ZnO is much weaker than that of ZnO:In sample. The reason for this difference is mainly coming from In doping. Indium in ZnO:In nanorods acts as donor dopant, which will produce donor energy levels under the bottom of the conduction band. Shallow donor energy levels are ionized at room temperature and provide electron carriers. These electrons will strengthen the intensity of the surface built-in field. As a result, more photogenerated electron–hole pairs are separated efficiently, and the surface photovoltaic response intensity of ZnO:In is enhanced.

To investigate the spectral photoresponse of the ZnO:In/SiO_2/Si heterostructure, we measured the photocurrent spectra with different monochromatic excitation wavelengths as shown in Fig. 5. One interesting phenomenon is that the photosensitivity occurs almost entirely in the ultraviolet and visible wavelength range. The maximum intensity of photoresponse locates in the wavelength region from 350 to 600 nm. The photocurrent intensity of the In-doped heterostructure is higher apparently than that of undoped ZnO/SiO_2/Si heterostructure in all wavelength range. According to the great difference of these samples in photoresponse performance, In incorporation benefits significantly the enhancement of photocurrent. Because of In^{3+} acting as a donor to provide electron carrier, the conduction performance of the sample is improved. Moreover, ZnO:In/SiO_2/Si heterostructure has enhanced photon response in a wide wavelength range. This broad photon response phenomenon is beneficial to the photoelectric conversion for light-collecting photovoltaic devices.

The current–voltage (I–V) curve for ZnO:In/SiO_2/Si heterojunction is illustrated in Fig. 6. The rectifying behavior is observed clearly. In reverse bias, the initially low leakage current equals nearly to zero, and is followed by a rather soft breakdown. The I–V characteristic curve shows a very low turn-on voltage of ~ 0.5 V for the forward bias and an obvious reverse cut-off property with high reverse bias breakdown voltage of ~ -18 V.

Finally, the capability of photovoltaic response of the ZnO:In/SiO_2/Si heterojunction was also investigated. Figure 7 shows photocurrent–voltage characteristic for ZnO:In/SiO_2/Si heterojunction under 10 mW/cm^2 illumination by using a tungsten-halogen-lamp. Its open-circuit voltage is about 62 mV. The SiO_2 insulation layer (~ 200 nm) formed between the ZnO:In layer and Si. This insulation layer will prevent the recombination of photogenerated electron–hole pairs. Consequently, the forming of SiO_2 layer makes photogenerated carriers separate much efficiently, and enhanced open-circuit voltage is obtained. The lower short-circuit current can be ascribed to the higher series resistance of the thin film. The major reason should be attributed to size and alignment of these nanorods. According to the SEM photograph

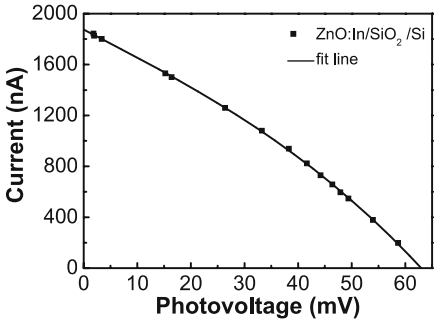

FIGURE 7 Current–photovoltage characteristic for ZnO:In/SiO_2/Si heterostructure

(Fig. 1), it can be observed that these ZnO:In nanorods do not align along one direction, which would reduce the conductance and mobility of the thin films. Growth of highly ordered and vertically aligned 2D and 1D ZnO nanoarrays will be expected to have enhanced carriers transport and improve the photoelectric conversion performance of the heterostructures photovoltaic device.

4 Conclusions

In summary, we fabricated ZnO:In nanorods on SiO_2/*n*-Si substrate in aqueous solution. The nanorods are characteristic hexagonal wurtzite structures. ZnO:In nanorods have a strong and broad UV surface photovoltage response. The ZnO:In nanorods/SiO_2/*n*-Si heterostructure photovoltaic device was prepared. The photoelectric conversion properties of the heterostructure were investigated. The heterostructure shows the rectifying current–voltage characteristics, and has a low turn-on voltage and a high breakdown voltage. ZnO:In/SiO_2/Si heterojunction has intense and wide photocurrent response in the UV-vis region. The photocurrent–voltage characteristic of the heterojunction was also investigated. It is very useful for nano-photoelectric conversion devices.

ACKNOWLEDGEMENTS This work is supported by the National Natural Science Foundation of China Grant Nos. 60376009 and 60278031, the Major Project of the National Natural Science Foundation of China Grant No. 60336020, and the Cultivation Fund of the Key Scientific and Technical Innovation Project, Ministry of Education of China No.704017.

REFERENCES

1 L.W. Yang, X.L. Wu, G.S. Huang, T. Qiu, Y.M. Yang, J. Appl. Phys. **97**, 014 308 (2005)
2 P.X. Gao, Z.L. Wang, J. Appl. Phys. **97**, 044 304 (2005)
3 H.C. Hsu, C.Y. Wu, W.F. Hsieh, J. Appl. Phys. **97**, 064 315 (2005)
4 W.I. Park, Y.H. Jun, S.W. Jung, G.C. Yi, Appl. Phys. Lett. **82**, 964 (2003)
5 W.I. Park, G.C. Yi, M. Kim, S.J. Pennycook, Adv. Mater. (Weinheim) **15**, 1841 (2002)
6 B. Sun, H. Sirringhaus, Nano Lett. **5**, 2408 (2005)
7 L.E. Greene, M. Law, D.H. Tan, M. Montano, J. Goldberger, G. Somorjai, P. Yang, Nano Lett. **5**, 1231 (2005)
8 L. Stolt, J. Hedström, J. Kessler, M. Ruckh, K.O. Velthaus, H.W. Schock, Appl. Phys. Lett. **62**, 597 (1993)
9 A. Gupta, A.D. Compaan, Appl. Phys. Lett. **85**, 684 (2004)
10 M.A. Green, S.R. Wenham, Appl. Phys. Lett. **65**, 2907 (1994)
11 C. Heske, U. Groh, L. Weinhardt, O. Fuchs, B. Holder, E. Umbach, C. Bostedt, L.J. Terminello, S. Zweigart, T.P. Niesen, F. Karg, Appl. Phys. Lett. **81**, 4550 (2002)
12 G. Ganguly, D.E. Carlson, S.S. Hegedus, D. Ryan, R.G. Gordon, D. Pang, R.C. Reedy, Appl. Phys. Lett. **85**, 479 (2004)
13 T. Yoshida, H. Minoura, Adv. Mater. (Weinheim) **12**, 1219 (2000)
14 L. Vayssieres, Adv. Mater. (Weinheim) **15**, 464 (2003)
15 Y.H. Lin, D.J. Wang, Q.D. Zhao, J. Phys. Chem. B **108**, 3202 (2004)
16 B.S. Li, L. Liu, Z.Z. Zhi, D.Z. Shen, Y.M. Lu, J.Y. Zhang, X.G. Kong, X.W. Fan, Thin Solid Films **414**, 170 (2002)
17 A.E. Rakhshani, Solid State Electron. **29**, 7 (1986)
18 E. Burstein, Phys. Rev. **93**, 632 (1954)
19 I. Hamberg, C.G. Granqvist, J. Appl. Phys. **60**, R123 (1986)
20 K.L. Chopra, S. Major, D.K. Pandya, Thin Solid Films **102**, 1 (1983)
21 L. Kronik, Y. Shapira, Surf. Sci. Rep. **37**, 1 (1999)